

## Evolution of strain throughout gallium nitride deposited on silicon carbide

M.A. Mastro<sup>a</sup>, N.D. Bassim<sup>a</sup>, J.A. Freitas Jr.<sup>a</sup>, M.E. Twigg<sup>a</sup>, C.R. Eddy Jr.<sup>a</sup>, D.K. Gaskill<sup>a</sup>, R.L. Henry<sup>a</sup>, R.T. Holm<sup>a</sup>, J. Kim<sup>b,\*</sup>, P.G. Neudeck<sup>c</sup>, A.J. Trunek<sup>d</sup> and J.A. Powell<sup>e</sup>

<sup>a</sup>Electronic Science and Technology Division, US Naval Research Laboratory, Washington, DC 20375

<sup>b</sup>Department of Chemical and Biological Engineering, Korea University, Seoul Korea

<sup>c</sup>NASA Glenn Research Center, Cleveland, Ohio 44135

<sup>d</sup>OAI, Cleveland, Ohio 44135

<sup>e</sup>Sest Inc., Cleveland, Ohio 44135

During GaN growth on an on-axis SiC substrate, a large density of dislocations ( $\sim 10^9 \text{ cm}^{-2}$ ) is unavoidably generated by the GaN/SiC misfit, uncontrolled misorientation in the substrate and defects present at the surface of the substrate. Recently a unique SiC substrate was developed with step-free and stepped mesas as well as continuous surface areas similar to a standard wafer all in close proximity. It is now possible to isolate the influence of defects and steps on the deposition of GaN on SiC. This paper provides a link between the dislocation environment and the strain state in the GaN film as well as the change of this strain with increasing thickness.

**Key words:** Gallium Nitride, Silicon Carbide, Strain, Growth.

### Introduction

Currently, the most widespread technique to produce III-nitride thin films is via metal organic chemical vapor deposition (MOCVD) on sapphire and SiC substrates [1, 2]. Unfortunately, this heteroepitaxy generates a density of dislocations ( $> 10^8 \text{ cm}^{-2}$ ) that essentially prohibits the operation of certain optoelectronic devices such as ultra-violet (UV) light emitting diodes, UV and blue laser diodes, and UV photovoltaics as well as some III-nitride electronic devices such as vertical bipolar transistors [3, 4]. The two commercial techniques used to produce GaN with dislocation densities less than  $10^7 \text{ cm}^{-2}$  are epitaxial lateral overgrowth and deposition on pseudo-bulk substrates grown by hydride vapor phase epitaxy [5-7]. Both routes are prohibitively expensive except in the production of laser diodes and, additionally, the configuration of epitaxial lateral overgrowth prevents the design of vertical or large area devices.

SiC is a favored substrate for deposition of GaN based solely on its high thermal conductivity, hexagonal crystal structure and relative availability, however, the lack of progress in heteroepitaxy of low-dislocation GaN is naively attributed primarily to the lattice parameter difference ( $-3.2\%$ ) and coefficient of thermal expansion mismatch ( $+16\%$ ) with SiC [1, 2, 7-11]. Growth of GaN directly on SiC is difficult due to the energetics

of the SiC surface, thus an AlN buffer layer is inserted prior to deposition of the GaN layer. Deposition of the AlN buffer layer is characteristic of a Stranski-Krastanov (S-K) growth mode in which the film coherently grows up to a critical thickness of approximately 4 nm at which point the excess total strain in the film favors the subsequent formation of AlN islands that nucleate and coalesce [12, 13]. The initial stages of AlN growth are under compression due to the lattice mismatch with the SiC substrate. Consequently, most of the lattice mismatch with SiC is absorbed in the first few nm of AlN deposition. The subsequent growth of GaN on AlN follows a similar SK growth mode where the thickness of the coherent GaN layer is typically 1 to 5 bilayers due to the small (2.5%) mismatch between GaN and AlN [12-17]. As a result, the lattice mismatch between GaN and SiC is absorbed in the AlN and the first nm of the GaN layers via defect generation. This defect creation mechanism, however, does not account for the high level of dislocations ( $10^9$  to  $10^{10} \text{ cm}^{-2}$ ) often measured in GaN films on SiC. Nucleation of GaN islands was observed at undulations in the AlN surface with threading dislocations related to this nucleation event. It has been proposed that these undulations in the AlN layer are mostly due to defects in the SiC surface [12].

This islanding in the SK mode creates  $10^6 \text{ cm}^{-2}$  to  $10^{11} \text{ cm}^{-2}$  nuclei (or growth islands) similar to the Volmer Weber (VW) growth mode [18]. The angular deviation of growth islands is dependent on the misfit, offset and presence of defects in the substrate. Similar to VW growth, during SK growth the nuclei will grow both vertically and laterally until they intersect each other

\*Corresponding author:  
Tel : +82-2-3290-3291  
Fax: +82-2-926-6102  
E-mail: jhkim@prosys.korea.ac.kr

and at this point the nuclei will snap (or zipper) together [19]. Because islands are firmly connected to the substrate, this zipping will lead to a rapid increase in tensile stress in the film that is dependent on the grain size by [20]:

$$\sigma_g = 0.683 (c_{11} + c_{12} - 2c_{13}^2/c_{33}) \varepsilon = 307.1 \text{ GPa } \Delta/d_0 \quad (1)$$

where  $d_0$  is the grain diameter,  $\Delta$  is the gap distance,  $\varepsilon = \Delta/d_0$  is the strain due to the gap closure process.

The structure possesses a large tensile intrinsic stress at the point when the film becomes continuous. It is common for a film grown beyond this point to experience a compressive stress associated with one or more dislocation annihilation mechanisms [21]. The proportional influence of this compressive stress on the net stress locally and in the entire film can vary based on the structure of the system and the availability of energetically favorable dislocation annihilation mechanisms. In our case, following an extension of Cammarata et al. [21], annihilation of threading dislocations with increasing thickness leads to an effective increase in pristine crystal (grain) size. Accordingly this densification introduces an intrinsic compressive stress into the film [22]. This stress contribution is described by [23]:

$$\sigma_t = \eta Y \delta (1/d_0 - 1/d_t) \quad (2)$$

where  $1/d_0$  is the dislocation density at coalescence,  $\delta$  is the excess volume per unit area associated with the defect-free crystal,  $\eta$  is a geometric factor that depends on the shape of the defect-free crystal.

Edwards et al. observed the compressive/tensile/weak tensile (or compressive) transitions described above for GaN growth on SiC with the peak in tensile stress observed at approximately 1  $\mu\text{m}$  of film thickness [24]. The absolute stresses generated at the growth temperature are less tensile (or more compressive) than that measured at room temperature by reason of the thermal expansion mismatch stress between GaN and SiC, nevertheless the general trend is the same. Additionally, Edwards et al. found that GaN films were under more tensile strain when grown on offcut SiC compared to on-axis SiC [24]. Their conjecture - despite their acknowledged contradiction to the experimental findings - was that the presence of surface steps provided sites for dislocation formation that would locally reduce the stress in the film. More in concordance with this report as well as the work of Edwards et al. [24] is a high density of dislocations generated at the initial stages of growth would create a high density of nuclei that generates a proportional tensile stress in the film [equation (1)].

The opposite limiting case would be to investigate the growth of GaN on an atomically-flat step-free SiC surface. Until the recent work of Neudeck et al. such a surface did not exist on SiC of any appreciable area [8]. In this paper, three cases will be investigated: high,

intermediate and low rates of dislocation annihilation in GaN grown on defective, stepped and step-free SiC, respectively.

A technique was developed to deposit heteroepitaxial films of 3C-SiC [8, 9] and, more recently, GaN [10] with low dislocation densities ( $<10^7 \text{ cm}^{-2}$ ) on step-free SiC mesas. Square mesas up to 200  $\mu\text{m}$  on a side were etched into an on-axis 4H-SiC wafer to isolate growth surface areas of SiC from other regions containing axial screw dislocations. Prior to SiC epitaxial growth, the surface of the mesas or any on-axis wafer will unavoidably contain atomic steps due to mis-alignments in the cut and polishing of the wafer. Moreover, the curvature of the SiC crystal planes due to the large build-up of residual stress generated during sublimation growth of SiC ingots only exacerbates this problem [11].

A pure step-flow SiC chemical vapor deposition (CVD) growth process was developed to extend all the atomic scale crystallographic steps on a given mesa to the periphery, leaving behind a step-free and atomically flat (0001) 4H-SiC surface [9]. In a properly optimized SiC mesa growth process, a clear distinction between step-free, stepped and highly defective SiC mesas is readily observed via optical microscopy due to the evolution of thin SiC cantilevers as illustrated in Neudeck et al. [8]. The difference in width of the step-free and stepped mesas typically fell between 5-8%. Using TEM, Bassim et al. determined the density of threading edge dislocations to be approximately  $5 \times 10^7 \text{ cm}^{-2}$  and despite exhaustive analysis, they observed no threading screw dislocations after 1  $\mu\text{m}$  of GaN growth [10].

## Experiments

In this study, GaN layers were grown by MOCVD on 4H-SiC mesas with and without surface steps arrayed across the same substrate as well as on the so-called defective continuous layers in trenches adjacent to the mesas. Growth was carried out in a modified vertical impinging flow CVD reactor. 4H-SiC wafers were cleaned in TCE, acetone, methanol for 5 minutes each in an ultrasonic bath, followed by HF submersion for 5 s, then blown dry in  $\text{N}_2$ . An Al seed layer was deposited prior to the onset of  $\text{NH}_3$  flow to protect the 4H-SiC surface and to prevent the formation of a discontinuous silicon nitride layer. A 100 nm AlN buffer layer was deposited at 1050  $^\circ\text{C}$  and 50 Torr (6.7 kPa). Subsequently, a 3  $\mu\text{m}$  GaN structure was deposited at 1020  $^\circ\text{C}$  and 250 Torr (33 kPa). In-situ reflectance from a 534.5 nm wavelength HeNe laser was used to monitor the growth process in real time. Micro-Raman-scattering measurements were performed at room temperature with the 488 nm line of an  $\text{Ar}^+$  ion laser. Further details of the growth process and equipment are available elsewhere [25].

## Results and Discussions

The identification of stepped and step-free mesas is possible with optical microscopy as shown in Fig. 1. The SiC step-flow growth mode is designed to extend every step in the SiC surface to the periphery of the mesa. This high horizontal growth rate creates cantilevers that extend over edge of the original mesa as is also observable in Fig. 2. SiC stepped mesas are created via an incoherent step-flow (step-bunching) mechanism that exists due to the existence of screw dislocations that continually source steps and thus prohibit step-flow growth to the edge of the mesa. Statistically a certain number of mesas will contain defects such as micropipes, poly-type inclusions or even large particulates. These highly defective mesas are easily identified with optical microscopy and are

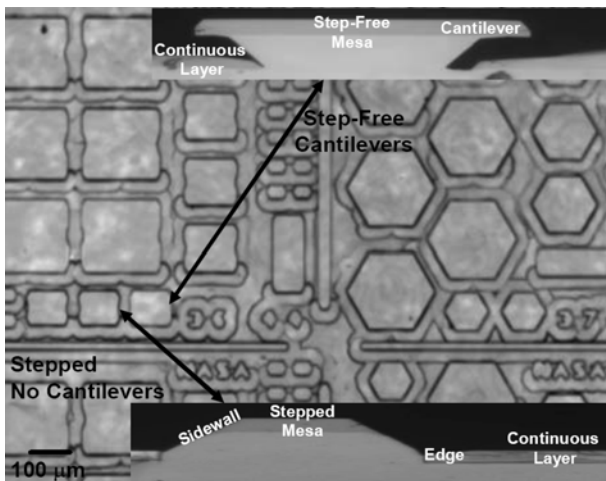


**Fig. 1.** Plan view optical picture of the patterned surface. The SiC pure step-flow growth creates cantilevers that are observable as small wings on the mesas. The inserts display cross-sectional optical pictures of their respective step-free or stepped mesa. The high horizontal growth rate in the SiC as well as GaN is observable in the cross-sectional picture of the step-free mesa.

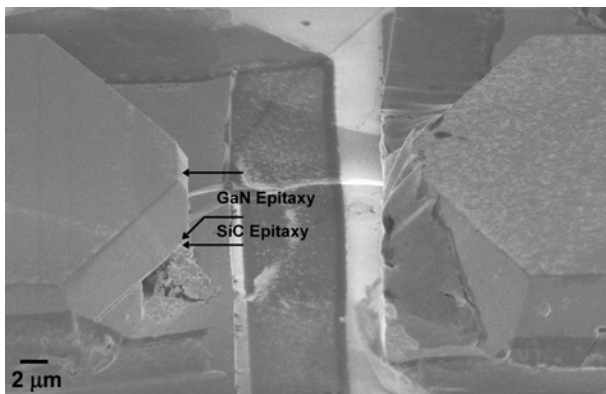


**Fig. 2.** Electron micrograph of a GaN film on step-free (left) and stepped (right) SiC mesas. The cantilever on the left mesa is indicative of step-free growth. Note the rough surface of the GaN film on the stepped mesa (right) particularly when compared to the smooth GaN film on the step-free mesa (left).

excluded in this study. Lastly, the areas between the mesas will be identified as continuous as they experience a growth environment similar to that of a continuous GaN layer on an unpatterned SiC substrate. To minimize error, structural comparisons with a mesa will be made with continuous layers immediately adjacent to the mesa.

Micro-Raman characterization was employed to investigate the strain-state of GaN at different points in the film with an approximate 1  $\mu\text{m}$  resolution (Fig. 3). A shift to shorter wavenumbers indicates a stretching of the III-nitride bonds due to a tensile stress in the layer. The wavenumber shift to stress relation was reported to be about 2.9  $\text{cm}^{-1}/\text{GPa}$  for GaN [26]. The GaN near the interface with the step-free mesa displayed a peak at 567.7  $\text{cm}^{-1}$ , which corresponds to a tensile stress of 103.4 MPa. This tensile strain reduced (or compressive strain increased) slightly ( $\Delta\sigma=69$  MPa) with increasing thickness. Comparatively, the GaN on the stepped mesa displayed a moderately larger tensile stress of 172 MPa near the interface with a slightly greater rate of tensile strain reduction ( $\Delta\sigma=103$  MPa) with increasing thickness. The strain in the continuous GaN near the mesas was recorded to provide a qualitative strain comparison with GaN on mesas. The continuous GaN at the SiC interface was strained by 482 MPa near the stepped mesa and 620 MPa near the step-free mesa. This high tensile strain state was rapidly reduced by 207 and 310 MPa over the next 2  $\mu\text{m}$  of growth near the stepped and step-free mesas, respectively.

This study of GaN growth on these dissimilar SiC surfaces provides a unique insight into the development of the dislocation environment and strain in GaN. It is known that threading dislocations annihilate with increasing growth thickness in many semiconductors.

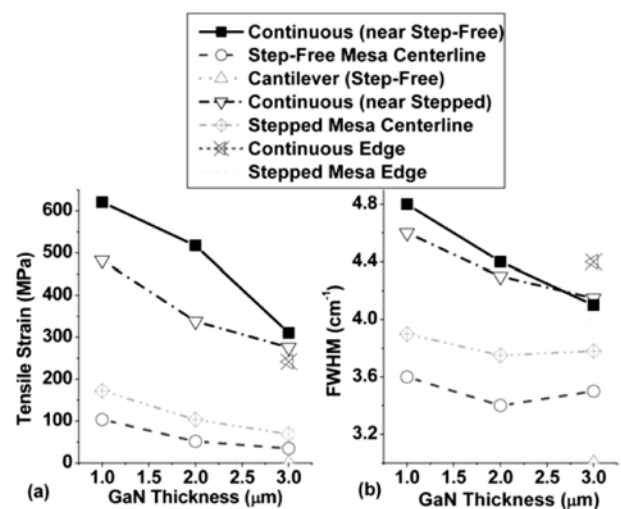


**Fig. 3.** Strain (a) and FWHM (b) of GaN deposited by MOCVD on SiC step-free and stepped mesas as well as in continuous areas surrounding the mesa. The rate of strain reduction is greatest in the continuous layers while this rate of change is the least in the step-free GaN. Note that the edge of the GaN cantilever is essentially strain free.

In GaN deposition, the dislocation density is inversely related to film thickness by :

$$\rho_{td}=1/h^n, \quad (3)$$

where  $h$  is the film thickness and  $n$  varies depending on the material system with  $n=0.66$  in a study of thick GaN on sapphire by Mathis et al. [27]. It is possible to measure the strain state of GaN at various locations in a thick layer, however, this strain state does not correlate to a change in dislocation density, rather the strain state is related to macroscopic bowing particularly when the film thickness approaches the thickness of the substrate.

Comparatively, in this study, the unique substrate with step-free, stepped and continuous surface areas in close proximity reveals in the GaN epitaxial layer a large dissimilarity in initial strain state and evolution of this strain with increasing thickness. A detailed investigation of this microstructure of similar films has been reported elsewhere [10] and is in progress on the sample examined in this paper [28]; the relevant points of which are presented below.

The continuous GaN layer behaves as is typical for a GaN layer grown on large area SiC substrate. During the initial stages of growth, a large density of defects ( $\sim 10^{12} \text{ cm}^{-2}$ ) is generated due to misfit with the substrate. Additional screw-type threading dislocations are generated by step edges as well as a screw-island growth mechanism instigated by macro-defects present at the substrate surface. The distortion of the continuous GaN crystal near the interface with SiC is observable in Fig. 3. The high tensile stress within the first  $1 \mu\text{m}$  of growth is presumably due to the generation of a small-grain structure with a high density of dislocations intersecting the nuclei. Similarly, the large FWHM of the Raman signal is emblematic of severe tilt and twist in the film. The high dislocation density provides an effective route for densification and thus compressive strain with increasing film thickness via annihilation of threading dislocations through a slip plane [22, 23]. This increase in compressive strain was the highest for the continuous GaN layers due to the high initial dislocation density as is predicted by equations (1), (2) and (3).

The GaN grown on stepped mesas is mainly controlled by the misfit with and the presence of step edges in the substrate. Additionally, the presence of step edges has been shown to create a periodic set of screw dislocations via the Nagai tilt mechanism [29]. Electron microscopy in Bassim et al. [10] measured a relatively low dislocation density of approximately  $10^8 \text{ cm}^{-2}$  for GaN grown on stepped mesas. A similar trend is observed again for this structure as Fig. 3 displays a moderate level of tensile strain within the first  $1 \mu\text{m}$  of growth and corresponding moderate rate of tensile strain reduction with increasing thickness.

Comparatively, epitaxy on step-free mesas isolates

the role of misfit in film deposition. Related studies of step-free GaN revealed a remarkable absence of vertical threading dislocation generation [10] as well as the formation of dislocation annihilation pathways that are typically obscured in highly defective films [28]. Transmission electron microscopy found that after  $1 \mu\text{m}$  of GaN growth on step-free mesas that the density of threading edge dislocations was approximately  $5 \times 10^7 \text{ cm}^{-2}$  and the density of threading screw dislocations was zero within the entire mesa width [30]. The resolution of the micro-Raman system used in this analysis is limited to approximately  $1 \mu\text{m}$  thus it is not possible to measure strain in the nuclei deposited close to the substrate. Nevertheless, Fig. 3 suggests that a high quality film with a low density of dislocations has a lower rate change, i.e., driving force, to a lower strain state.

Growth on mesa structures is also advantageous as it localizes strain to the particular mesa. Normally such strains in a large-area continuous layer will bend the entire substrate [31, 32]. By removing the horizontal constraint of a continuous film, the strain in each mesa is effectively isolated [4, 30].

## Conclusion

In summary, the development of strain in GaN films on SiC has been investigated. A comparison of GaN epitaxy on three different SiC surfaces revealed the strong influence of defects and step edges on the evolution of strain in the GaN.

## Acknowledgements

Research at the Naval Research Lab is supported by Office of Naval Research. Research at Korea University was supported by the Korea Research Foundation Grant funded by the Korean Government (MOEHRD) (KRF-2006-331-D00126).

## References

1. M. Henini, and M. Razeghi, *Optoelectronic Devices: III Nitrides*, Elsevier Science, Berlin (2005).
2. M.A. Mastro, D.V. Tsvetkov, V.A. Soukhoveev, A. Usikov, V. Dmitriev, B. Luo, F. Ren, K.H. Baik, and S.J. Pearton, *Solid State Electronics* 48 (2004) 179-182.
3. M.A. Mastro, J.R. LaRoche, N.D. Bassim, and C.R. Eddy, Jr. *Microelectronics Journal* 36 (2005) 705-711.
4. M.A. Mastro, C.R. Eddy Jr.; N.D. Bassim; M.E. Twigg; R.L. Henry; R.T. Holm, and A. Edwards, *Solid State Electronics* 49[2] (2005) 251-256.
5. O. Kryliouk, M. Reed, M. Mastro, T. Anderson, and B. Chai, *Phys. Stat. Solidi A* 176-1 (1999) 407-410.
6. M.D. Reed, O.M. Kryliouk, M.A. Mastro, and T.J. Anderson, *J. Crystal Growth* 274 (2005) 14-20.
7. S. Nakamura, G. Fasol, and S.J. Pearton, *The Blue Laser Diode: The Complete Story*, Springer, Berlin (2000).
8. P.G. Neudeck, J.A. Powell, G.M. Beheim, E.L. Benavage, P.B. Abel, A.J. Trunek, D.J. Spry, M. Dudley, and W.M.

- Vetter, J. Appl. Phys. 92 (2002) 2391-2400.
9. J.A. Powell, P.G. Neudeck, A.J. Trunek, G.M. Beheim, L.G. Matus, R.W. Hoffman, and L.J. Keys, Appl. Phys. Lett. 77 (2000) 1449-1451.
  10. N.D. Bassim, M.E. Twigg, C.R. Eddy Jr., J.C. Culbertson, M.A. Mastro, R.L. Henry, R.T. Holm, P.G. Neudeck, A.J. Trunek, and J.A. Powell, Appl. Phys. Lett. 86 (2005) 21902-1~21902-3.
  11. R.S. Okojie and M. Zhang, in *Materials Research Society Symposium*, edited by M. Dudley, P. Gouma, T. Kimoto, P. G. Neudeck, and S.E. Saddow (Materials Research Society, Warrendale, PA, 2004), Vol. 815, pp. 133-138.
  12. R.F. Davis, S. Einfeldt, E.A. Preble, A.M. Roskowski, Z.J. Reitmeier, P.Q. Miraglia, Acta Materialia 51(2003) 5961-5979.
  13. S. Tanaka, R.S. Kern, and R.F. Davis, Appl. Phys. Lett. 66 (1995) 37-39.
  14. N. Grandjean, and J. Massies, Appl. Phys. Lett. 71 (1997) 1816-1818.
  15. B. Damilano, N. Grandjean, F. Semond, J. Massies, and M. Leroux, Appl. Phys. Lett. 75 (1999) 962-964.
  16. D.D. Koleske, M.E. Twigg, J.C. Culbertson, R.L. Henry, A.E. Wickenden, M. Fatemi, and S.C. Binari, Phys. Stat. Sol. A 183 (2001) 184-187.
  17. M.E. Twigg, R.L. Henry, A.E. Wickende, D.D. Koleske, and J.C. Culbertson, Appl. Phys. Lett. 75 (1999) 686-688.
  18. H.J. Scheel, "Control of Epitaxial Growth Modes of High-Performance Devices" in *Crystal Growth Technology*, Ed. H.J. Scheel and T. Fukuda, John Wiley and Sons (2003).
  19. J.A. Floror, E. Chason, R.C. Cammarato, and D.J. Srolovitz, MRS Bulletin 27[1] (2002) 19-21.
  20. T. Bottcher, S. Einfeldt, S. Figge, R. Chierchia, H. Heinke, D. Hommel, and J.S. Speck, Appl. Phys Lett. 78 (2001) 1976-1978.
  21. R.C. Cammarata, T.M. Trimble, and D.J. Srolovitz, J. Mater. Res. 15[11] (2000) 2468-2474.
  22. P. Chaudhari, J. Vac. Sci. Technol. 9 (1972) 520-522.
  23. M.F. Doerner, and W.D. Nix, CRC Crit Rev. Sol. State Mater. Sci. 14 (1988) 225-234.
  24. N.V. Edwards, M.D. Bremser, R.F. Davis, A.D. Batcher, S.D. Yoo, C.F. Karan, and D.E. Aspnes, Appl. Phys. Lett. 73 (1998) 2808-2810.
  25. C.R. Eddy Jr., R.T. Holm, R.L. Henry, J.C. Culbertson, and M.E. Twigg, J. Elec. Mat. 34[9] (2005) 1187-1192.
  26. M. Kuball, Surf. Interface Anal. 31 (2001) 987-999.
  27. S.K. Mathis, A.E. Romanov, L.F. Chem, G.E. Beltz, W. Pompe, and J.S. Speck, J. Cryst. Growth 231 (2001) 371-390.
  28. N.D. Bassim, M.E. Twigg, M.A. Mastro, C.R. Eddy, Jr., T.J. Zega, R.L. Henry, J.C. Culbertson, R.T. Holm, P. Neudeck, J.A. Powell, A.J. Trunek, J. Cryst. Growth (In Press)
  29. X.R. Huang, J. Bai, M. Dudley, B. Wagner, R.F. Davis, Y. Zhu, Phys. Rev. Letts. 95 (2005) 086101-1~086101-4.
  30. N.D. Bassim, M.E. Twigg, C.R. Eddy, Jr., R.L. Henry, R.T. Holm, J.C. Culbertson, R.E. Stahlbush, P.G. Neudeck, A. J. Trunek, and J.A. Powell, Appl. Phys. Lett. 84 (2004) 5216-5218.
  31. J. Torvik, M. Leksono, J. Pankove, and B. Van Zegbroeck, MRS Internet J. Nitride Semicond. Res. 4 (1999) 3-8.
  32. M.A. Mastro, M. Fatemi, D.K. Gaskill, K-K. Lew, B.L. Van Mil, C.R. Eddy Jr., and C.E.C. Wood, J. Appl. Phys. 100 (2006) 093510-1~093510-5.